15th Triennial World Congress, Barcelona, Spain

POWER PLANT COORDINATED-CONTROL WITH WIDE-RANGE CONTROL-LOOP INTERACTION COMPENSATION

Raul Garduno-Ramirez[a] and Kwang Y. Lee[b]

[a] *Division of Control Systems, GCI, Electrical Research Institute, Temixco, Mor. 62490 Mexico*
[b] *Department of Electrical Engineering, The Pennsylvania State University, University Park, PA 16802 USA*

Abstract: A coordinated-control scheme with a compensator for a fossil-fuel power plant is presented. The compensator is intended to reduce the interaction effects among the control loops to ease control during wide-range normal operating conditions. Placed between the controllers and the power plant, the compensator only introduces compensation factors among the control signals; preserving the direct control loop paths of the original control scheme. The compensation factors can be determined from an equivalent process gain matrix. Analysis shows that the proposed compensation is numerically well-conditioned, and simulation experiments show that it effectively handles control loop interaction throughout the power plant operation range. *Copyright © 2002 IFAC*

Keywords: Power plants, Coordinated-control, Wide-range normal operation, Control-loop interaction, Relative gain array, Interaction compensation, Decoupling control.

1. INTRODUCTION

Typically, a fossil-fuel power unit (FFPU) is required to provide fast and stable power supply during load changes and load disturbances. The thermal energy provided by the boiler must equalize, at all times, the energy needed by the steam turbine and the electric generator to match the electric load. Hence, the main duty of the coordinated-control (CC) scheme is to match the slow response of the boiler with the faster turbo-generator response to ease power generation for load tracking under normal operation conditions.

Current CC schemes consist of multiple single-input-single-output feedback control loops, which evaluate conventional PI or PID algorithms. These schemes have shown their adequacy for power regulation, but can be seriously challenged by wide-range operation requirements, such as load-following for frequency regulation in a power system. In these conditions, the FFPU performance may significantly decrease due to the nonlinear coupled process dynamics. To reduce or to eliminate the effects of control loop interaction, the basic CC configuration has been complemented with many different compensation schemes (Taft, 1987, Dimeo, and Lee, 1995). However, with a few exceptions (Ray and Majumder, 1985), the design of most compensation schemes is not systematic, but heavily relies on the designer's experience, nor the resulting schemes are good for wide-range operation.

This paper introduces a CC scheme that eases power generation for wide-range load-tracking under normal operation conditions. The scheme consists of a three-loop augmented CC and a feedforward compensator that effectively reduces the interaction among the control loops throughout the FFPU operation range. The interaction compensator (IC) is systematically designed using an equivalent process gain matrix, which is obtained through interaction analysis based on the relative gain array technique (McAvoy, 1983). Section 2 presents the FFPU models to be used in the following sections. Section 3 introduces the proposed CC+IC control scheme. Section 4 presents the design procedure for the IC and demonstrates its feasibility. Section 5 presents results of wide-range load-tracking simulations. Finally, Section 6 concludes this work.

2. POWER PLANT MODELS

2.1 Power Unit Nonlinear Model

The essential dynamics of a FFPU for overall wide-range simulations have been remarkably captured for an 160 MW oil fired drum-type unit through a third order nonlinear model (Bell and Astrom, 1987). The inputs are the positions of valve actuators that control the mass flow rates of fuel (u_1 in pu), steam to the turbine (u_2 in pu), and feedwater to the drum (u_3 in pu). The three outputs are electric power (E in MW),

drum steam pressure (P in kg/cm^2), and drum water level deviation (L in m). The three state variables are electric power, drum steam pressure, and the steam-water density (ρ_f). The state equations are:

$$\frac{dE}{dt} = \left((0.73u_2 - 0.16)P^{9/8} - E\right)/10 \quad (1a)$$

$$\frac{dP}{dt} = 0.9u_1 - 0.0018u_2P^{9/8} - 0.15u_3 \quad (1b)$$

$$\frac{d\rho_f}{dt} = (141u_3 - (1.1u_2 - 0.19)P)/V_t \quad (1c)$$

The drum water level output is calculated with the following algebraic equations:

$$q_e = (0.85u_2 - 0.14)P + 45.59u_1 - 2.51u_3 - 2.09 \quad (2a)$$

$$\alpha_s = (1/\rho_f - 0.0015)/(1/(0.8P - 25.6) - 0.0015) \quad (2b)$$

$$L = 50(0.13\rho_f + 60\alpha_s + 0.11q_e - 65.5) \quad (2c)$$

where α_s is the steam quality, and q_e is the evaporation rate (kg/sec). The positions of the valve actuators are constrained to [0,1].

Equations (1) and (2) constitute a nonlinear model:

$$\begin{aligned} \dot{x} &= f(x,u) \\ y &= g(x,u) \end{aligned} \quad (3)$$

where $x = [x_1\ x_2\ x_3]^T = [E\ P\ \rho]^T$ is the state vector, $u = [u_1\ u_2\ u_3]^T$ is the input vector, and $y = [y_1\ y_2\ y_3]^T = [E\ P\ L]^T$ is the output vector.

2.2 State-Space Model

A linear state-space model can be obtained from the Taylor series expansion of the nonlinear equations (3) around an equilibrium point defined by $x_e = [x_{1e}\ x_{2e}\ x_{3e}]^T$ and $u_e = [u_{1e}\ u_{2e}\ u_{3e}]^T$ with $y_e = [y_{1e}\ y_{2e}\ y_{3e}]^T$ as the corresponding output. The linear model matrices are given by:

$$\begin{aligned} A &= \left.\frac{\partial f}{\partial x}\right|_{x_e,u_e}, \quad B = \left.\frac{\partial f}{\partial u}\right|_{x_e,u_e}, \\ C &= \left.\frac{\partial g}{\partial x}\right|_{x_e,u_e}, \quad D = \left.\frac{\partial g}{\partial u}\right|_{x_e,u_e} \end{aligned} \quad (4)$$

Then, the linear model approximation is given by:

$$\dot{\hat{x}} = A\hat{x} + B\hat{u} \quad , \quad \hat{y} = C\hat{x} + D\hat{u} \quad (5)$$

where $\hat{x} = x - x_e$, $\hat{u} = u - u_e$, and $\hat{y} = y - y_e$ are the state, input, and output vector deviations, respectively. Hence, the system matrices are:

$$A = \begin{bmatrix} -0.1 & \frac{9}{8}(0.073u_{2e} - 0.016)x_{2e}^{1/8} & 0 \\ 0 & -\frac{9}{8}0.0018u_{2e}x_{2e}^{1/8} & 0 \\ 0 & -0.0118(1.1u_{2e} - 0.19) & 0 \end{bmatrix} \quad (6a)$$

$$B = \begin{bmatrix} 0 & 0.073x_{2e}^{9/8} & 0 \\ 0.9 & -0.0018x_{2e}^{9/8} & -0.15 \\ 0 & -0.0129x_{2e} & 1.6588 \end{bmatrix} \quad (6b)$$

$$C = \begin{bmatrix} 1 & 0 & 0 \\ 0 & 1 & 0 \\ 0 & C_{32} & C_{33} \end{bmatrix} \quad (6c)$$

$$D = \begin{bmatrix} 0 & 0 & 0 \\ 0 & 0 & 0 \\ 253.29 & 4.7423x_{2e} & 13.967 \end{bmatrix} \quad (6d)$$

where:

$$\begin{aligned} C_{32} &= \frac{2400/x_{3e} - 3.6912}{(1.0394 - 0.0012x_{2e})^2} + 16.5229(1.1u_{2e} - 0.19) \\ C_{33} &= 6.5365 - \frac{2400x_{2e} - 76800}{(1.0394 - 0.0012x_{2e})x_{3e}^2} \end{aligned} \quad (7)$$

2.3 Transfer Matrix Model

The transfer matrix model can be obtained directly from the linear state-space model in the previous section using the Laplace transform:

$$\hat{Y} = T\ \ \hat{U} = \left[C(sI - A)^{-1}B + D\right]\ \hat{U} \quad (8)$$

where $\hat{Y}$ and $\hat{U}$ are the Laplace transform of the output deviation, $\hat{y}$, and the input deviation, $\hat{u}$, s is the Laplace complex variable, and T stands for the system transfer matrix. The elements of the transfer function matrix are found to be:

$$\begin{aligned} T_{11} &= [A_{12}B_{21}s] / d(s) \\ T_{12} &= [B_{12}s^2 + (A_{12}B_{22} - A_{22}B_{12})s] / d(s) \\ T_{13} &= [A_{12}B_{23}s] / d(s) \\ T_{21} &= [B_{21}s^2 - A_{11}B_{21}s] / d(s) \\ T_{22} &= [B_{22}s^2 - A_{11}B_{22}s] / d(s) \\ T_{23} &= [B_{23}s^2 - A_{11}B_{23}s] / d(s) \\ T_{31} &= [D_{31}s^3 + (B_{21}C_{32} - D_{31}(A_{11} + A_{22}))s^2 + \\ &\quad ((A_{32}C_{33} - A_{11}C_{32})B_{21} + D_{31}A_{11}A_{22})s] / d(s) \\ T_{32} &= [D_{32}s^3 + (B_{22}C_{32} + B_{32}C_{33} - D_{32}(A_{11} + A_{22}))s^2 \\ &\quad + (A_{11}A_{22}D_{32} - A_{11}B_{22}C_{32} + A_{32}B_{22}C_{33} - (A_{11} \\ &\quad + A_{22})B_{32}C_{33})s + (A_{11}A_{22}B_{32}C_{33} - \\ &\quad A_{11}A_{32}B_{22}C_{33})] / d(s) \\ T_{33} &= [D_{33}s^3 + (B_{23}C_{32} + B_{33}C_{33} - D_{33}(A_{11} + A_{22}))s^2 \\ &\quad + (A_{11}A_{22}D_{33} - A_{11}B_{23}C_{32} + A_{32}B_{23}C_{33} - (A_{11} \\ &\quad + A_{22})B_{33}C_{33})s + (A_{11}A_{22}B_{33}C_{33} - \\ &\quad A_{11}A_{32}B_{23}C_{33})] / d(s) \end{aligned} \quad (9)$$

where

$$d(s) = s(s - A_{11})(s - A_{22}) = s_3 - (A_{11} + A_{22})s^2 + A_{11}A_{22}s \quad (10)$$

3. CONTROLLER CONFIGURATION

The CC strategies were introduced to capture the fast and stable response characteristics of formerly developed simpler strategies, without any of their disadvantages. To attain fast response, the turbo-

generator is allowed to use the thermal energy stored in the boiler. To achieve stability, the boiler control adjusts the fuel firing rate according to the required power, keeping the turbine from exceeding the energy provided by the boiler. To this aim, the unit load demand is simultaneously routed to both the boiler and the turbine controls, i.e., in an actual CC scheme, the control signal for the fuel/air valves is provided by the load controller from the unit load demand and the measured power, while the control signal for the throttle valve is provided by the pressure controller from the measured throttle steam pressure and the pressure set-point, which is obtained from the unit load demand through a non-linear mapping (Fig. 1).

The proposed CC + IC scheme updates the conventional CC strategy in two steps (Fig. 2). First, from the fact that in a drum-type FFPU the electric power and steam pressure are tightly coupled and are affected heavily by the fuel/air flow and the steam flow, and that the feedwater flow slighly affects power and pressure, but greatly affects the drum water level, the typical power-pressure CC strategy is augmented with the drum water level control loop. With this approach, internal energy balanced operation can be achieved at any load in the entire FFPU operation range, which is a major need to be satisfied for effective wide-range operation. Second, an IC is inserted between the controllers and the FFPU. The objective of this addition is to provide a way to deal with the interaction effects among the feedback control loops along the whole operation range of the FFPU. It is expected that the IC will decrease the interaction effects at levels that are easily manageable by the controllers with lessened control effort.

4. INTERACTION DECOUPLER DESIGN

This section shows the design of the IC in two stages. First, the design is carried out for a single operating point. Then, the results are shown for the entire power unit operation range. For any given operating point, the IC is designed as a static decoupling compensator, that is, instead of using the process dynamic transfer functions, only the steady-state gain of the process transfer functions are used.

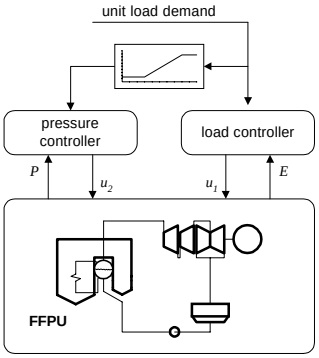

Fig. 1. Conventional coordinated-control.

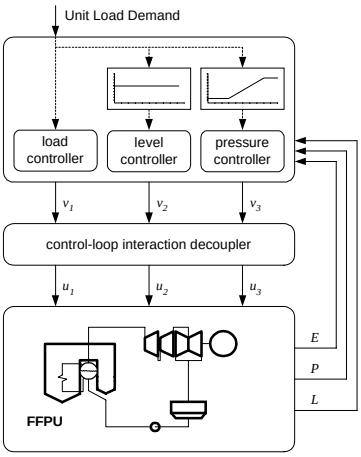

Fig. 2. Coordinated-control with compensator.

The main advantages of static, or steady-state, decoupling are that the design involves rather simple numerical computations, the resulting compensators are always realizable, and the design only requires knowledge of the process steady-state gain matrix, which may be calculated from experimental steady-state input-output process data.

4.1 Design Procedure

Regarding its development, the IC takes into account the best characteristics of the three main decoupling approaches (Luyben, 1970). First, design is carried out as in the simplified decoupling case. Then, the realization is made as with the inverse decoupling structure. Finally, the resulting IC equates the fully decoupled apparent transfer functions of the ideal decoupling case in steady-state conditions. The IC structure is shown in Fig. 3.

The simplified decoupling approach, in the steady-state case, requires the product of the process steady-state gain matrix *K*:

$$K = \lim_{s \to 0} T(s) \tag{11}$$

and the interaction compensator matrix *D* to be equal to a decoupled steady-state gain matrix *M* satisfying:

$$\begin{bmatrix} M_1 & 0 & 0 \\ 0 & M_2 & 0 \\ 0 & 0 & M_3 \end{bmatrix} = \begin{bmatrix} K_{11} & K_{12} & K_{13} \\ K_{21} & K_{22} & K_{23} \\ K_{31} & K_{32} & K_{33} \end{bmatrix} \begin{bmatrix} 1 & D_{12} & D_{13} \\ D_{21} & 1 & D_{23} \\ D_{31} & D_{32} & 1 \end{bmatrix} \tag{12}$$

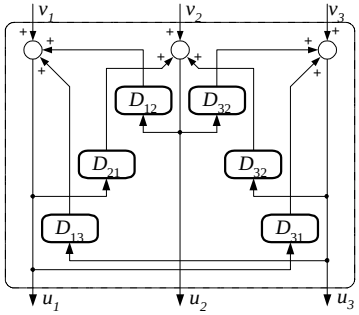

Fig. 3. Control-loop interaction compensator.

where the D_{ij}, i=1,2,3, j=1,2,3, forming matrix D, are the decoupling factors, or interaction compensation factors, to be determined, and the M_1, M_2, and M_3, forming matrix M, are the decoupled steady-state gains for the power, pressure, and level control loops, respectively. Carrying out the product on the right hand side of (12), and equating to zero the resulting off-diagonal elements, yields the system of equations:

$$\begin{aligned} 0 &= K_{21} + K_{22}D_{21} + K_{23}D_{31} \\ 0 &= K_{31} + K_{32}D_{21} + K_{33}D_{31} \\ 0 &= K_{11}D_{12} + K_{12} + K_{13}D_{32} \\ 0 &= K_{31}D_{12} + K_{32} + K_{33}D_{32} \\ 0 &= K_{11}D_{13} + K_{12}D_{23} + K_{13} \\ 0 &= K_{21}D_{13} + K_{22}D_{23} + K_{23} \end{aligned} \tag{13}$$

which can be solved simultaneously, by pairs, giving:

$$\begin{aligned} D_{21} &= \frac{K_{23}K_{31} - K_{21}K_{33}}{K_{22}K_{33} - K_{23}K_{32}} \\ D_{31} &= \frac{K_{21}K_{32} - K_{22}K_{31}}{K_{22}K_{33} - K_{23}K_{32}} \\ D_{12} &= \frac{K_{13}K_{32} - K_{12}K_{33}}{K_{11}K_{33} - K_{13}K_{31}} \\ D_{32} &= \frac{K_{12}K_{31} - K_{11}K_{32}}{K_{11}K_{33} - K_{13}K_{31}} \\ D_{13} &= \frac{K_{12}K_{23} - K_{13}K_{22}}{K_{11}K_{22} - K_{12}K_{21}} \\ D_{23} &= \frac{K_{13}K_{21} - K_{11}K_{23}}{K_{11}K_{22} - K_{12}K_{21}} \end{aligned} \tag{14}$$

Relations in (14) define the interaction compensator, with steady-state decoupled process gains:

$$M_1=K_{11} \ , \quad M_2=K_{22} \ , \quad M_3=K_{33} \tag{15}$$

4.2 Wide-Range Interaction Compensation

For the FFPU case, the main problem in the above procedure to calculate the decoupling factors is to know the steady-state gain matrix (11). The inclusion of the the drum water level control loop, to extend the scope of the of the CC scheme to achieve wide-range operation, adds in integrative process dynamics, for which steady-state gain becomes undetermined. This problem makes it difficult to quantify control loop interaction to provide any reasonable compensation. However, interaction analysis based on the relative gain array (RGA) method shows that the interaction information provided by the process steady-state gain matrix can also be retrieved from an equivalent gain matrix (McAvoy, 1983). Thus, the equivalent gain matrix can be utilized to design the compensator following the same procedure.

From (11) and (9), the elements of the process steady-state gain matrix K are calculated as:

$$\begin{aligned} K_{11} &= \lim_{s\to 0} T_{11}(s) = \frac{A_{12}B_{21}}{A_{11}A_{22}} \\ K_{12} &= \lim_{s\to 0} T_{12}(s) = \frac{A_{12}B_{22} - A_{22}B_{12}}{A_{11}A_{22}} \\ K_{13} &= \lim_{s\to 0} T_{13}(s) = \frac{A_{12}B_{23}}{A_{11}A_{22}} \\ K_{21} &= \lim_{s\to 0} T_{21}(s) = -\frac{B_{21}}{A_{22}} \\ K_{22} &= \lim_{s\to 0} T_{22}(s) = -\frac{B_{22}}{A_{22}} \\ K_{23} &= \lim_{s\to 0} T_{23}(s) = -\frac{B_{23}}{A_{22}} \\ K_{31} &= \lim_{s\to 0} T_{31}(s) = \lim_{s\to 0}\left(-\frac{A_{32}B_{21}C_{33}}{sA_{22}} \right) \\ &= \lim_{s\to 0}\frac{\gamma_{31}}{s} \\ K_{32} &= \lim_{s\to 0} T_{32}(s) = \lim_{s\to 0}\left(\frac{A_{22}B_{32}C_{33} - A_{32}B_{22}C_{33}}{sA_{22}} \right) \\ &= \lim_{s\to 0}\frac{\gamma_{32}}{s} \\ K_{33} &= \lim_{s\to 0} T_{33}(s) = \lim_{s\to 0}\left(\frac{A_{22}B_{33}C_{33} - A_{32}B_{23}C_{33}}{sA_{22}} \right) \\ &= \lim_{s\to 0}\frac{\gamma_{33}}{s} \end{aligned} \tag{16}$$

where γ_{31}, γ_{32}, and γ_{33}, are appropriately defined for the equalities to hold. Because of K_{31}, K_{32}, and K_{33}, the steady-state matrix K is undetermined. This voids direct calculation of the RGA through the Hadamard product (element by element):

$$\Lambda = \left(K^{-1}\right)^T * K \tag{17}$$

Fortunately, there is a simple mechanism to calculate the RGA in these cases. Matrix K may be written as:

$$\begin{aligned} K &= \lim_{s\to 0}\begin{bmatrix} K_{11} & K_{12} & K_{13} \\ K_{21} & K_{22} & K_{23} \\ \dfrac{\gamma_{31}}{s} & \dfrac{\gamma_{32}}{s} & \dfrac{\gamma_{33}}{s} \end{bmatrix} \\ &= \lim_{s\to 0}\begin{bmatrix} 1 & 0 & 0 \\ 0 & 1 & 0 \\ 0 & 0 & \dfrac{1}{s} \end{bmatrix}\begin{bmatrix} K_{11} & K_{12} & K_{13} \\ K_{21} & K_{22} & K_{23} \\ \gamma_{31} & \gamma_{32} & \gamma_{33} \end{bmatrix} \end{aligned} \tag{18}$$

then,

$$K^{-1} = \lim_{s\to 0}\begin{bmatrix} K_{11} & K_{12} & K_{13} \\ K_{21} & K_{22} & K_{23} \\ \gamma_{31} & \gamma_{32} & \gamma_{33} \end{bmatrix}^{-1}\begin{bmatrix} 1 & 0 & 0 \\ 0 & 1 & 0 \\ 0 & 0 & s \end{bmatrix} \tag{19}$$

Introducing L, appropriately defined:

$$K^{-1} = \lim_{s\to 0} \begin{bmatrix} L_{11} & L_{12} & L_{13} \\ L_{21} & L_{22} & L_{23} \\ L_{31} & L_{32} & L_{33} \end{bmatrix} \begin{bmatrix} 1 & 0 & 0 \\ 0 & 1 & 0 \\ 0 & 0 & s \end{bmatrix} = \lim_{s\to 0} \begin{bmatrix} L_{11} & L_{12} & L_{13}s \\ L_{21} & L_{22} & L_{23}s \\ L_{31} & L_{32} & L_{33}s \end{bmatrix} \quad (20)$$

The RGA is obtained from (18) and (20) taking the Hadamard product, canceling *s*, and taking the limit:

$$\Lambda = \begin{bmatrix} L_{11}K_{11} & L_{21}K_{12} & L_{31}K_{13} \\ L_{12}K_{21} & L_{22}K_{22} & L_{32}K_{23} \\ L_{13}\gamma_{31} & L_{23}\gamma_{32} & L_{33}\gamma_{33} \end{bmatrix} \quad (21)$$

which would be the same if *K* was simply given by:

$$K = \begin{bmatrix} K_{11} & K_{12} & K_{13} \\ K_{21} & K_{22} & K_{23} \\ \gamma_{31} & \gamma_{32} & \gamma_{33} \end{bmatrix} \quad (22)$$

Hence, (22) can be taken as the FFPU equivalent steady-state gain matrix to design the interaction compensator following the procedure in Section 4.1.

As a numerical example, Table 1 presents decoupling factors for the entire FFPU operation range along a typical sliding pressure operation policy. In the next two sections, the adequacy of the CC+IC scheme for wide-range operation is demonstrated by analyzing the numerical feasibility and sensitivity of the IC along the same operation policy.

Table 1. Compensator elements

E_d	P_d	D_{12}	D_{13}	D_{21}	D_{23}	D_{31}	D_{32}
20	38.2	-0.085	0.239	3.96	0.00	1.22	0.006
40	50.7	-0.077	0.239	2.91	0.00	1.19	0.020
60	63.2	-0.082	0.239	2.29	0.00	1.17	0.029
80	75.8	-0.092	0.239	1.88	0.00	1.15	0.038
100	88.3	-0.102	0.239	1.59	0.00	1.13	0.046
120	100.8	-0.115	0.239	1.37	0.00	1.12	0.054
140	113.3	-0.127	0.239	1.21	0.00	1.11	0.061
160	125.8	-0.141	0.239	1.08	0.00	1.10	0.069

4.3 Numerical Feasibility

Analyzing the numerical characteristics of the steady-state gain matrix may assess the feasibility of the interaction compensator. With that aim, designing the interaction compensator is equivalent to solve the system of linear equations:

$$y = Ku = Mv \quad (23)$$

for the process input vector, *u*, in terms of the control signal vector, *v*:

$$u = K^{-1}Mv = Dv \quad (24)$$

Clearly, if *K* is degenerate, decoupling will be extremely difficult to achieve, and if *K* is not full-rank decoupling can not be achieved. Degeneracy of matrix *K* can be assessed through the condition number, which is the single most reliable indicator of the conditioning of a matrix. The condition number is defined as the ratio of the largest to the smallest singular value of the gain matrix:

$$cn = \frac{\bar{\sigma}\ (K)}{\underline{\sigma}\ (K)} \quad (25)$$

The larger the condition number (>100), the poorer the numerical conditioning of the matrix, that is, the larger its degeneracy. Fig. 4 shows the condition number along the typical sliding pressure operation policy defined in table 1. It can be seen that the gain matrix does not degenerates. Thus, the compensator may be confidently designed.

4.4 Numerical Sensitivity

After the feasibility of the interaction compensator has been established, another closely related issue to examine is its sensitivity to modeling errors, since no process model is 100% accurate. In this regard, consider an error ΔK in the estimate of the steady-state gain matrix:

$$y = (K + \Delta K)\, u \quad (26)$$

The compensator *D*, designed in terms of *K*, yields:

$$y = (K + \Delta K)\, Dv = (K + \Delta K)K^{-1}Mv \quad (27)$$

where the amount of error introduced into *y* due to the model mismatch is given by:

$$\Delta y = \Delta K K^{-1} M v \quad (28)$$

that can be rewritten using the definition of the inverse of a matrix as:

$$\Delta y = \frac{\Delta K Adj(K) M v}{|K|} \quad (29)$$

The output error Δy is inversely proportional to the determinant of the gain matrix, $|K|$. Fig. 5 shows $|K|$ along the typical sliding pressure operation policy defined in table 1. Clearly, it can be seen that the determinant is large enough to produce very small output deviations due to model errors; as required.

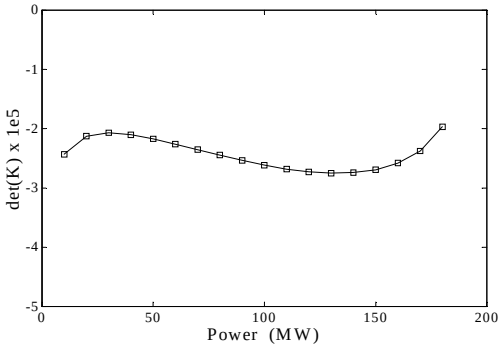

Fig. 4. Condition number of gain matrix.

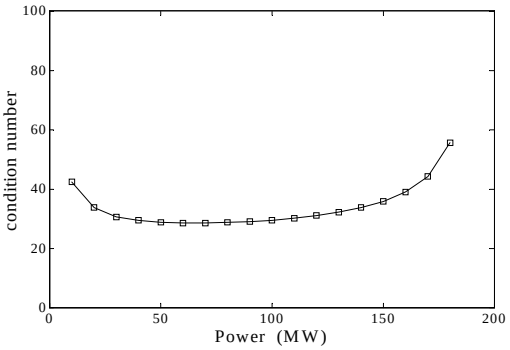

Fig. 5. Determinant of gain matrix.

5. SIMULATION RESULTS

Simulation experiments were carried out to evaluate the response of the power unit. Fig. 6 shows the unit response to a wide-range unit load demand ramp for both compensated and uncompensated cases. The ramp goes from 50% (80 MW) through 100% (160 MW) base load, with a 5%/min (8 MW/min) load rate, which is a rather fast loading according to american standards. Power and pressure responses are both good. However, a meaningful improvement is obtained in the compensated level response throughout the ramp transition, which means the compensator is effectively reducing the interaction among the control loops, thus helping the controllers to achieve their proposed goals.

6. CONCLUSIONS

A compound coordinated-control plus interaction compensator system for wide-range control of a FFPU was presented. Incorporation of the drum water level control loop into the coordinated control strategy is required to achieve wide-range balanced unit operation. Nevertheless, it challenged the design of the interaction compensator because of the integrative dynamics being introduced. The problem was solved using the RGA-based interaction analysis, which allowed building an equivalent steady-state gain matrix. Inclusion of the control-loop interaction compensator effectively reduced interaction among the feedback control loops, easing their job and improving their effectiveness throughout the FFPU operation range.

The interaction compensator was found to be numerically well-conditioned. The proposed design procedure is a systematic design approach that does not require the solution of an optimization problem, nor years of design experience. Furthermore, its structure provides the compensator with the versatility and necessary characteristics for practical application. Also, the fact that control loops with integrative dynamics can be included in the design without any further complication adds for the generality of the approach. It should be emphasized that this kind of process dynamics are normally avoided by other control strategies (*i.e.*, predictive

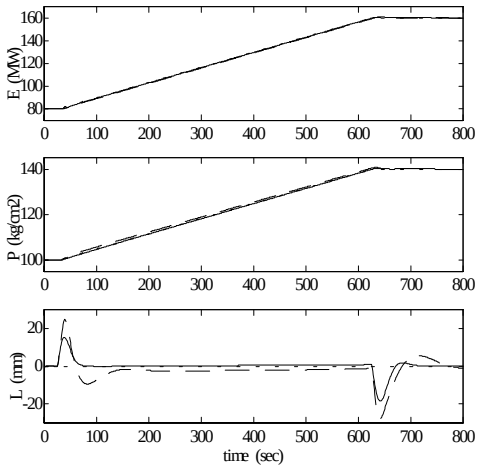

Fig. 6 Response to load ramp. Reference (dotted), uncompensated (dashed), compensated (solid).

control), thus making them less desirable for the development of overall control strategies.

Regarding the simplicity of the FFPU model being used for design, it is this characteristic which allowed getting insight into the control loop interaction problem. A follow up research will consider a more complete model for simulation experiments to better test the feasibility of the proposed scheme. Again, only normal operating conditions will be considered, since abnormal situations are commonly handled by other components of actual control systems.

7. ACKNOWLEDGMENTS

This work was supported in part by NSF under grants INT-9605028 and ECS-9705105, the Pennsylvania State University, the Electrical Research Institute (IIE), and Conacyt.

8. REFERENCES

Bell, R.D. and K.J. Astrom (1987). *Dynamic Models for Boiler-Turbine-Alternator Units: Data Logs and Parameter Estimation for a 160 MW Unit, TFRT-3192*. Lund Institute of Technology, Sweden.

Dimeo, R. and K.Y. Lee (1995). Boiler-turbine control system design using a genetic algorithm. *IEEE Trans. on Energy Conversion*. **10(4)**, 752-759.

Luyben, W.L. (1970). Distillation decoupling. *AIChE Journal.* **16(2)**, 198-203.

McAvoy, T.J. (1983). *Interaction Analysis*. Instrument Society of America. USA.

Ray, K.S. and D.D. Majumder (1985). Fuzzy logic control of a nonlinear multivariable steam generating unit using decoupling theory. *IEEE Trans. on Systems, Man, and Cybernetics*. **SMC-15(4)**, 539-558.

Taft, C.W. (1987). Performance evaluation of boiler control system strategies. *Proc. 1987 Conference on Control Systems for Fossil Fuel Power Plants*. **EPRI CS-6049**, 4-1/4-15.